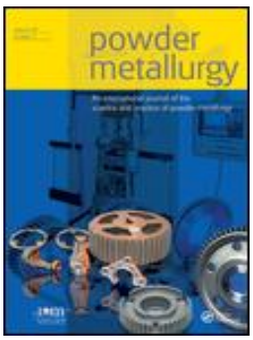

Powder Metallurgy

ISSN: (Print) (Online) Journal homepage: https://www.tandfonline.com/loi/ypom20

Fabrication and mechanical properties of Al–Si-based alloys by selective laser melting process

Yeong Seong Eom, Kyung Tae Kim, Dong Won Kim, Soo ho Jung, Jung Woo Nam, Dong Yeol Yang, Jungho Choe, Ji Hun Yu & Injoon Son

To cite this article: Yeong Seong Eom, Kyung Tae Kim, Dong Won Kim, Soo ho Jung, Jung Woo Nam, Dong Yeol Yang, Jungho Choe, Ji Hun Yu & Injoon Son (2021): Fabrication and mechanical properties of Al–Si-based alloys by selective laser melting process, Powder Metallurgy, DOI: 10.1080/00325899.2021.1899470

To link to this article: https://doi.org/10.1080/00325899.2021.1899470

Published online: 15 Mar 2021.

POWDER METALLURGY
https://doi.org/10.1080/00325899.2021.1899470

The Institute of Materials, Minerals and Mining

Taylor & Francis
Taylor & Francis Group

Fabrication and mechanical properties of Al–Si-based alloys by selective laser melting process

Yeong Seong Eom[a,b], Kyung Tae Kim[a], Dong Won Kim[a], Soo ho Jung[a], Jung Woo Nam[a,b], Dong Yeol Yang[a], Jungho Choe[a], Ji Hun Yu[a] and Injoon Son[b]

[a]Department for 3D Printing Materials, Korea Institute of Materials Science, Changwon-si, Republic of Korea; [b]Department of Metallurgical Engineering, Kyungpook National University, Bukgu, Republic of Korea

ABSTRACT

Aluminium (Al)-based alloys have attracted as promising materials for structural applications using metal 3D printing due to their excellent specific mechanical strength, formability, and durability. In this study, highly flowable coarse AlSi10Mg powders with average diameter of 65 μm were prepared and then they were additively manufactured by using the selective laser melting (SLM) process. The relative densities exceeding 99% were consistently obtained from the samples fabricated at the scan speed of 1000–2000 mm·s^{-1} in the range of laser power from 350 to 390 W. The tensile strengths and elongation of all the samples were characterised. Furthermore, Al alloy processed by coarse AlSi10Mg powders does not show a big change in strength values compared to those fabricated by fine AlSi10Mg powders with 45 μm in diameter. Thus, these results clearly show that the developed coarse AlSi10Mg powders can be effectively utilised for the SLM process.

ARTICLE HISTORY
Received 3 December 2020
Revised 26 February 2021
Accepted 2 March 2021

KEYWORDS
AlSi10Mg; powder size; additive manufacturing; SLM

1. Introduction

Additive Manufacturing process is a promising technology that manufactures three-dimensional objects by stacking materials using digitalised data, and is suitable for small quantity production of multi-species that meets increasingly diverse user needs. In recent years, it is being actively studied to utilise metal materials in the fields requiring high-strength complex structures such as automobiles, defense, aerospace, and medical parts [1,2]. Representative additive manufacturing for metal are classified by Directed Energy Deposition (DED) and Powder Bed Fusion (PBF) method, respectively. Particularly, the Selective Laser Melting (SLM) as one of PBF processes is known as effective method that can obtain a high-density 3D shape by melting metal powder using a high-power laser [3,4].

There have been many reports on the SLM process of stainless steel, nickel-based Inconel alloys, aluminium and even magnesium for high-strength structural applications [5–9]. Of those many metallic candidates, Al-based alloys have been actively researched in the transportation field such as automobiles and aviation because they can secure excellent mechanical properties, formability, and durability when manufactured as a 3D printed sculpture. However, in the case of Al-based materials, high-power laser equipment is necessarily required compared to other metals because of the oxide film on the surface and high reflectivity to the laser light [10]. Thus, development of the optimised SLM process of AlSi10Mg alloy powders have vigorously investigated and recently, the mechanical properties of SLMed bulks have deeply analysed [11–15]. However, compared to the casting method, the variation in properties among the SLMed samples is large and their elongation is relatively low due to inhomogeneous microstructures caused by rapid melting and solidification. Several researchers reported that the properties are modified by composition change using some additives such as Sr that help Si phase spheroidize [16,17]. Nonetheless, the commercialisation of AlSi10Mg alloy for high performance have limited because of the low productivity caused by the size of the powders under 45 μm. Fine powders do not often provide suitable flowability which is closely related to production rate of 3D product despite low energy density required to melt the powder. To obtain high spreadability or flowability of the AlSi10Mg powders is crucial to enhance productivity of 3D-printing process. Hence, there have been big needs for tuning on the size of AlSi10Mg powders for practical applications.

Thus, in this study, AlSi10Mg alloy powders with average diameter of 65 μm were prepared by gas atomiser system and then SLM process to the coarse powders was optimised to achieve highly densified bulk

CONTACT Kyung Tae Kim ktkim@kims.re.kr Department for 3D Printing Materials, Korea Institute of Materials Science, 797 Changwon-daero, Changwon-si, Gyeongnam 51508, Republic of Korea; Injoon Son ijson@knu.ac.kr Department of Metallurgical Engineering, Kyungpook National University, 80 Daehakro, Bukgu, Daegu 41566, Republic of Korea

materials. The microstructures and mechanical properties of the bulks are investigated. Furthermore, changes in tensile strength and elongation of the developed samples are compared with the stress-relief temperature. Finally, it was compared with the tensile properties of a sample made of fine powder having an average particle size of 25 μm.

2. Experimental procedure

2.1. Materials and methods

Coarse AlSi10Mg powders with average diameter of 65 μm used were prepared using a gas atomiser (PSI Co., UK). Table 1 shows the composition of AlSi10Mg powders fabricated in this study compared to commercial fine AlSi10Mg one. The synthesised powder was used to a selective laser melting (SLM) process using Concept Laser's M2 equipment (ytterbium fibre laser, 400 W). In order to overcome the oxide film on the surface of the Al alloy powder by completely melting the powder, the degree of overlap between the laser beams was fixed at 30% under the condition of laser power 350–390 W. The laser scan speed was changed up to 2800 mm·s^{-1}, and the laser scan pattern is a method of irradiating a laser by rotating 90 degrees each time the layer is raised. The atmosphere in the chamber where the process is performed was conducted under an argon atmosphere with an oxygen remaining amount of 0.1% to prevent oxidation of the sculpture. The shape of the sculpture was a plate and a cube ($10 \times 10 \times 10$ mm^3), and the plate-shaped sculpture was machined with a tensile sample according to ASTM E8/E8M subsize specimen. In addition, in order to check the mechanical properties change due to heat treatment, tensile samples with a laser power of 360 W and a scanning speed of 1600 mm·s^{-1} were heated up to 270, 300, and 330 °C at a rate of 10 °C·min^{-1} for 1 h. 30 min and then were air-cooled.

2.2. Characterisation

The powder size analysis of the AlSi10Mg powders for the 3D printing process was analysed under dry atmosphere conditions using Laser particle size analyzer (LS13, Beckman Coulter Co., USA). In order to measure the flow rate of the powder, 50 g of powder was put in a Hall flowmeter (Carney Funnel) and the flow time was measured.

Table 1. Comparison in composition of AlSi10Mg alloy powders for additive manufacturing.

	Al	Si	Mg	Mn	Fe	Sr
AlSi10Mg (commercial)	Balance	10.2	0.24	-	0.12	-
AlSi10Mg (In this study)	Balance	10.2	0.08	0.41	0.06	**0.01**

Relative densities of all samples were analysed by measuring the weight of the specimen by applying the Archimedes method. The surface morphology was analysed by OM (TME-BD, Nikon Co., Japan) and FE-SEM (MIRA3 LM, Tescan Co., Czech Republic). Etching for checking the microstructures was performed using a Keller reagent solution prepared by mixing HCl: HNO_3: HF: Distilled Water = 1.5: 2.5: 1: 95.

Tensile test were performed to obtain mechanical properties of machined three-dimensional objects by using a universal testing system (5982, Instron Co., USA) along with a strain rate of 0.25 mm·mm^{-1}·min^{-1}.

3. Results and discussion

Figure 1(a) shows a surface morphology of the AlSi10Mg powder synthesised in this study. The powder clearly shows a spherical shape and some of small powders are somewhat attached on the surface. Figure 1(b) exhibits the surface image enlarged to the powders which shows several particles with a few μm are attached onto the surface of the big powder. Figure 1 (c) shows the results of the powder size analysis for confirming the size distribution. The sizes corresponding to D_{10}, D_{50} and D_{90} are measured as 41, 65 and 99 μm, respectively. It was observed that small amount of powder with 10–30 μm in diameter are present. Figure 1(d) displays the XRD patterns showing clear Al and Si peaks as main phases.

Table 2 shows the comparison of physical properties of the synthesised AlSi10Mg powders compared to other powders [18]. As shown in Table 2, it was confirmed that the flowability slightly improved as the particle size increased from 25 to 65 μm. That is, while the flowability of 17.12 s is obtained from the particle size of 25 μm, 10.9 s is achieved from the coarse AlSi10Mg powder synthesised in this study. The Hausner ratio expressed as Tap density/Apparent density, is one of the characteristics representing the filling rate of the powder required for the production of the sculpture in the 3D printer chamber. The calculated value is also shown in Table 2. In general, the closer the Hausner ratio is to 1, the better the filling rate is expected. Although there is no obvious decrease in the Hausner ratio according to the particle size, it was confirmed that the coarse AlSi10Mg powder used in this study tends to show the lower value compared to the value of the conventional fine powder.

Figure 2(a) shows schematic fabrication plan of cubic samples for optimising suitable process parameters with relationship between laser power and laser scan speed. From left to right, the laser scan speed was changed from 700 to 2500 mm·s^{-1} and the laser scan power from bottom to top was changed to 350, 360, 370, 380 and 390 W. Figure 2(b) shows the

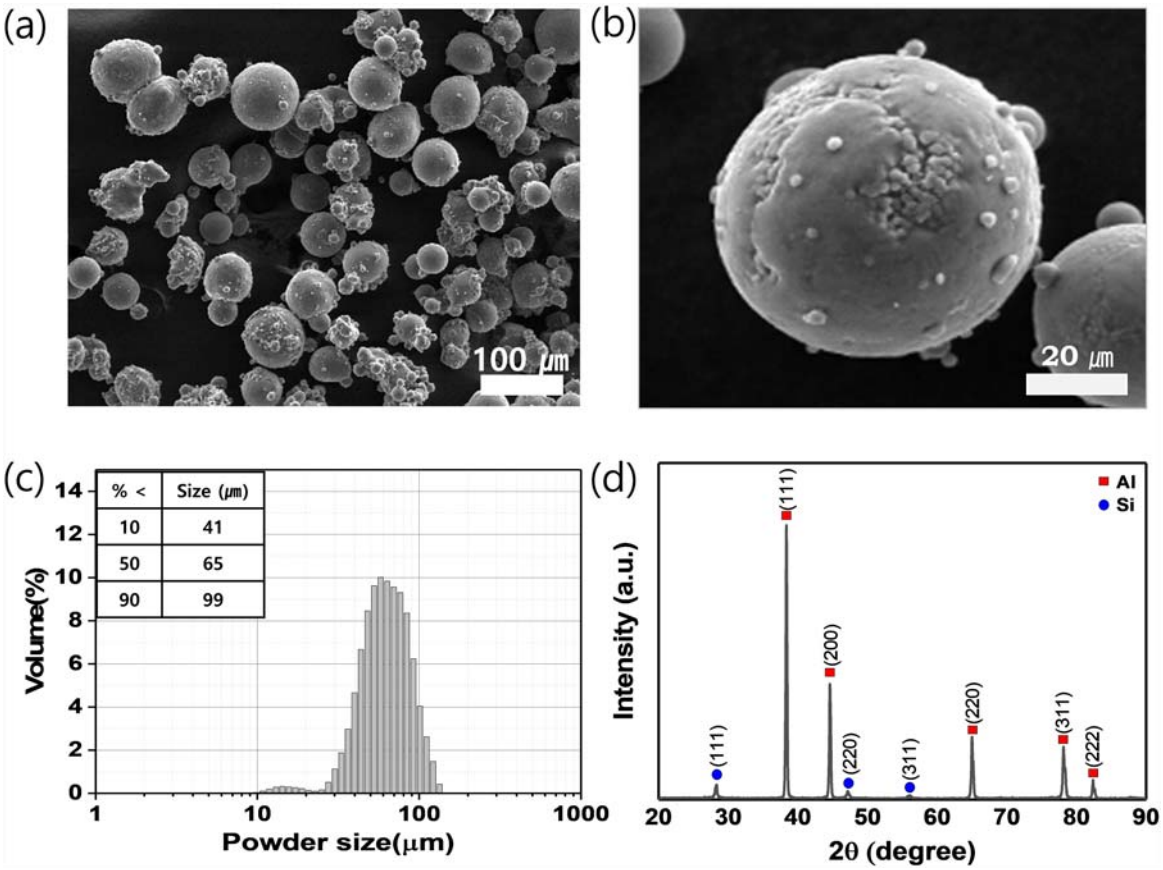

Figure 1. (a) Surface SEM image, (b) enlarged surface morphology, (c) powder size distribution and (d) XRD patterns of coarse AlSi10Mg powders prepared in this study.

result of the energy density corresponds to each sample by calculating the Equation (1) considering laser power and scan speed in the Figure 2(a). The energy density in SLM process can be calculated by following Equation (1).

$$\text{Energy density} = P/(v \cdot h \cdot t) \quad (1)$$

In the above equation, P is laser power, v is scan speed, h is hatch spacing, and t is layer thickness. Figure 2(c) shows a photograph of the cube samples fabricated according to the designed processing condition. Irregular surfaces caused by over-melting of the powder are observed at the condition under 700 mm·s^{-1} and over 370 W. This is analysed by high energy density that occurs when a high-capacity laser is slowly irradiated to the powders. High energy density of 143 J·mm^{-3} or more, results in a bumpy and rough surfaces. Based on this, the processing conditions are divided by three different maps in Figure 2 (b) which are overmelting region, normal melting region and unmalting region as energy density changes. That is, the orange-colored region is expected to correspond to over-melted areas and the green-colored region may be unmalting area.

Figure 2(d) shows relative density as a function of laser scan speed and the results are compared with laser power of 350, 360, 270, 380 and 390 W. Relative densities of most samples shows the values more than 99%, regardless of scan speed and laser power. Although we also checked the relative densities of the samples fabricated below 400 mm·s^{-1} and above 2800 mm·s^{-1}, the difference does not show big drop within 1%. These results indicate that the high relative density can be obtained from the condition of energy density of 40–110 J·mm^{-3} and this is useful information in the 3D printing of coarse AlSi10Mg powders.

Figure 3(a) shows schematic image of 3D printing and Figure 3(b) shows optical surface microstructures

Table 2. Comparison of physical properties of AlSi10Mg alloy powders for additive manufacturing process.

Sample	Average Powder Size (μm)	Flowability (Carney funnel) (sec/50 g)	Apparent density (g·cm^{-3})	Tap density (g·cm^{-3})	Hausner ratio
AlSi10Mg [18]	25	17.12	1.43	1.67	1.17
AlSi10Mg (commercial)	45	12.97	1.18	1.49	1.26
AlSi10Mg (In this study)	65	10.90	1.16	1.32	1.14

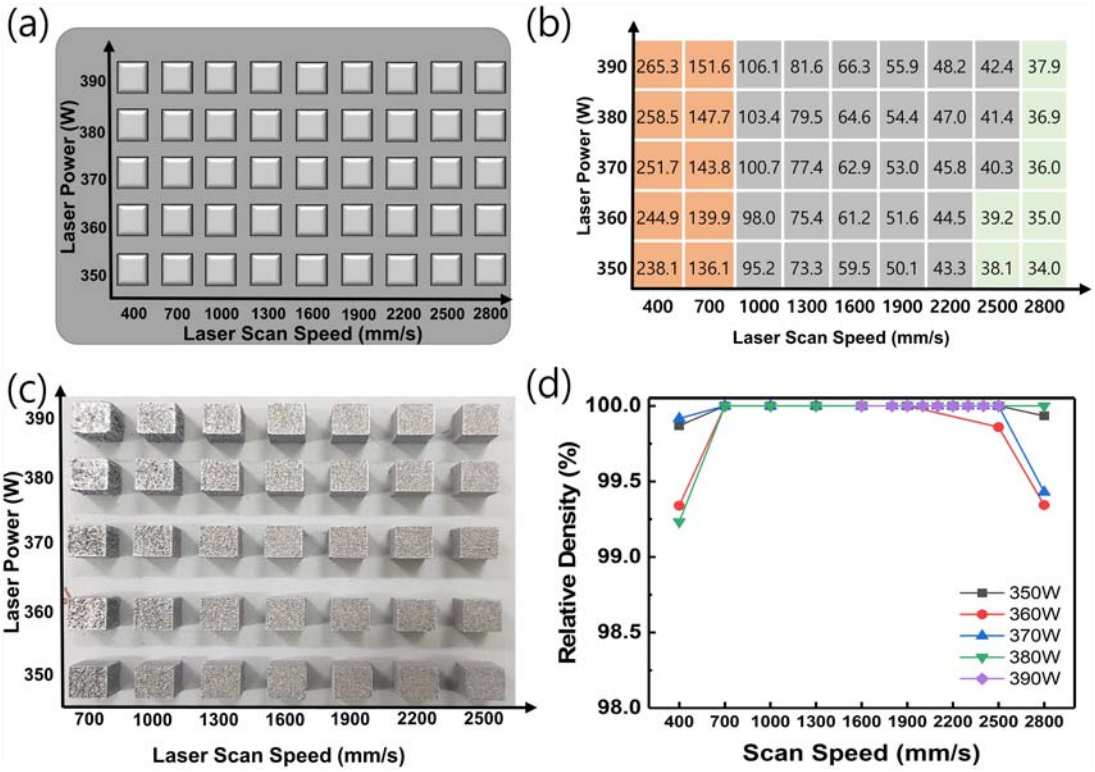

Figure 2. (a) Schematic diagram of designed processing map, (b) energy density corresponding to samples of (a), (c) fabricated samples with laser power and scan speed, and (d) relationship between relative density and laser scan speed of fabricated AlSi10Mg alloys using coarse powders.

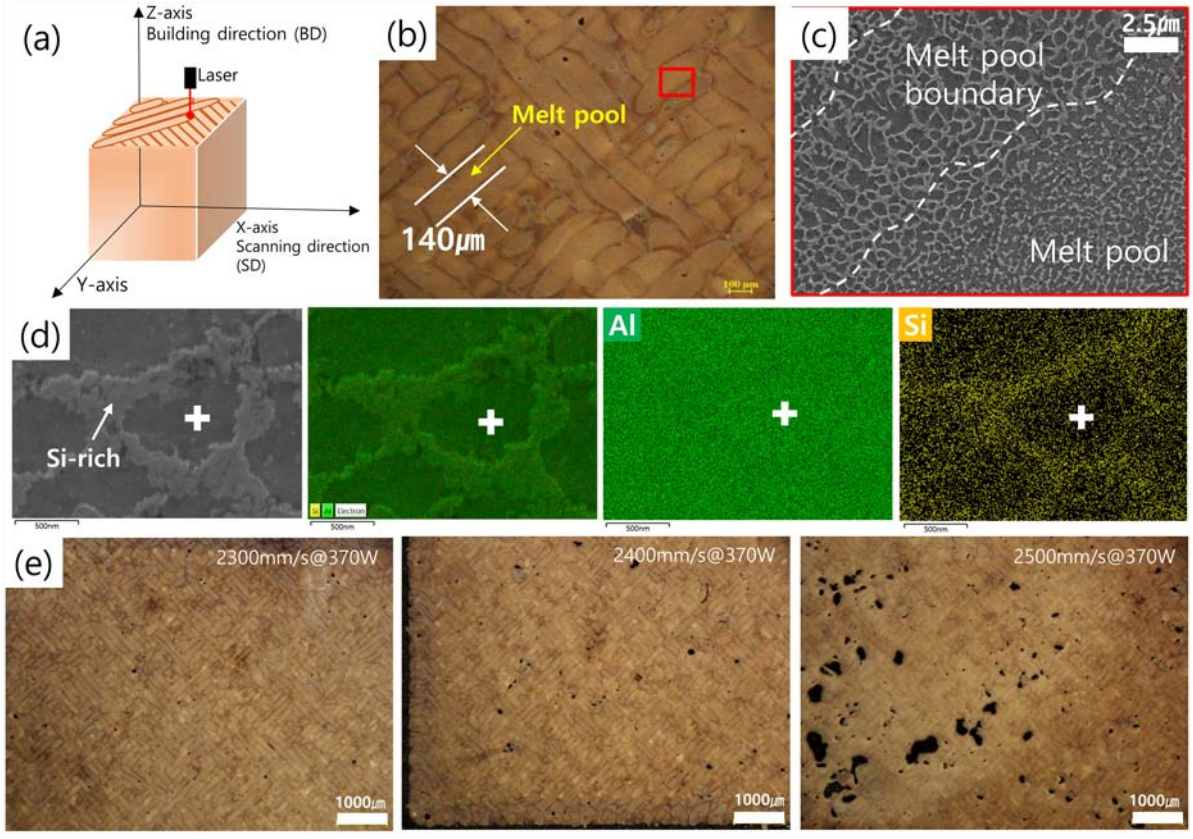

Figure 3. (a) Schematic illustration of fabricated cube sample, (b) optical surface image to reveal size of melt pool to perpendicular plane to building direction, (c) surface SEM image nearby melt pool boundary, (d) EDS results to show distribution of Al and Si element of fabricated AlSi10Mg alloys using coarse powders, and (e) OM images with different scan speed of 2300, 2400 and 2500 $mm{\cdot}s^{-1}$.

on building direction of the sample fabricated under the conditions of laser power 370 W, scan speed 2300 mm·s^{-1}. As shown in OM images, it was found that the melt pools are intersected with each other in a checkered pattern, because the laser is irradiated while rotating 90 degrees each time a layer is stacked. The average thickness of melt pool is measured approximately as 140 μm and the SEM observation to red-colored box region is displayed in Figure 3(c). Typical microstructure of 3D-printed Al–Si alloy that micrometre-scale Si-rich phases are connected in the Al matrix is observed. The EDS results in Figure 3(d) shows Si-rich phases are corresponding to the bright area. The Si-rich phases in melt pool are very homogeneously dispersed in the Al phases. Meanwhile, the Si-rich phases at the melt pool boundary are formed by coarse and good connectivity. Thanks to this uniform distribution of the Si-rich phase, it is possible to retain a higher strength than the mechanical strength of the cast alloy. The Si phase uniformly dispersed in the 3D-printed Al–Si alloy effectively hinders the movement of dislocations and improves the mechanical strength [19].

Figure 3(e) shows optical surface microstructures of the samples fabricated under the conditions of laser power 370 W, scan speed 2300, 2400 and 2500 mm·s^{-1}. The pores with a few tens of micrometer are started to clearly observe in the melt pool when the scan speed is over 2400 mm·s^{-1}. The formation of pores in melt pool can be typically determined by laser input energy. Micro CT analysis was performed to confirm the relationship between scan speed and pore.

Figure 4 displays the defects in the samples manufactured by 2300, 2400 and 2500 mm·s^{-1} at 370 W. Although the relative densities show the values over 99%, Micro CT reveals quantitative amount of defects as shown in Figure 4(a). The defect ratios per volume are measured about 1.25–2.34% despite their high relative densities. Figure 4(b) shows the information of the size and the number of defects in the samples. As scan speed increases by 2500 mm·s^{-1}, the size of the defects become 1.86 mm. Although total defect volumes are similar in three samples, the size of defects is obtained from the sample fabricated under rapid scan speed. The high-speed melting of the metal by the laser causes a droplet-shaped balling. Excessive balling results in an irregular surface, forming large pores [13]. As a result, the proportion of these large pores in size, affect lowering the mechanical performance, and thus the scan speed needs to be optimised.

Figure 5(a) shows a stress–strain curves with a laser power of 360 W and a laser scan speed of 1800 mm·s^{-1}. All the tensile samples are fractured without the severe cross-sectional reduction. The results of tensile strength of 460 MPa, yield strength of 279 MPa, and elongation of 9.4% showed high elongation at moderate tensile strength. Figure 5(b) shows the comparison of tensile strength test results according to scan speeds at the 360 W. Overall, there was no significant change in tensile strength as the scan speed was changed. In particular, it showed similar tensile strength values of about 440 MPa over a wide range of scan speeds from 1400 to 2200 mm·s^{-1}. Although scan speed can affect

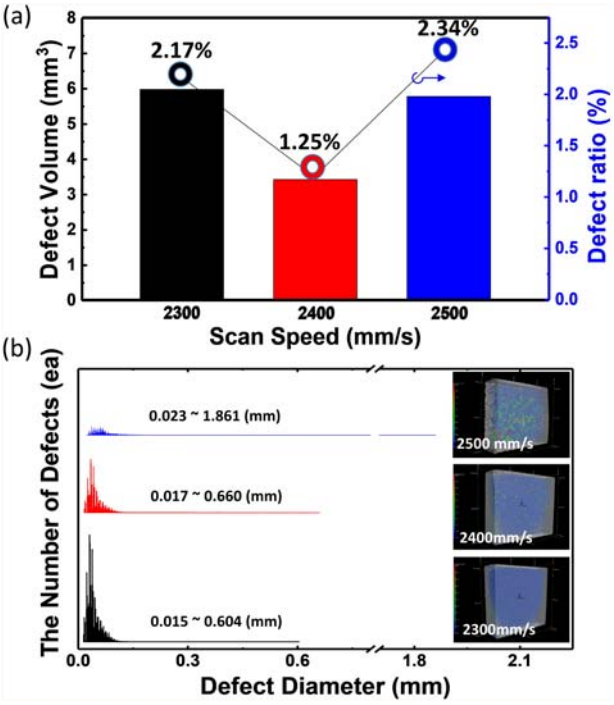

Figure 4. (a) Total defect volume and defect ratio per volume (b) the number of defects and defect diameter of the fabricated three samples with laser power of 370 W and scan speed of 2300, 2400 and 2500 mm·s^{-1} of fabricated AlSi10Mg alloys using coarse powders.

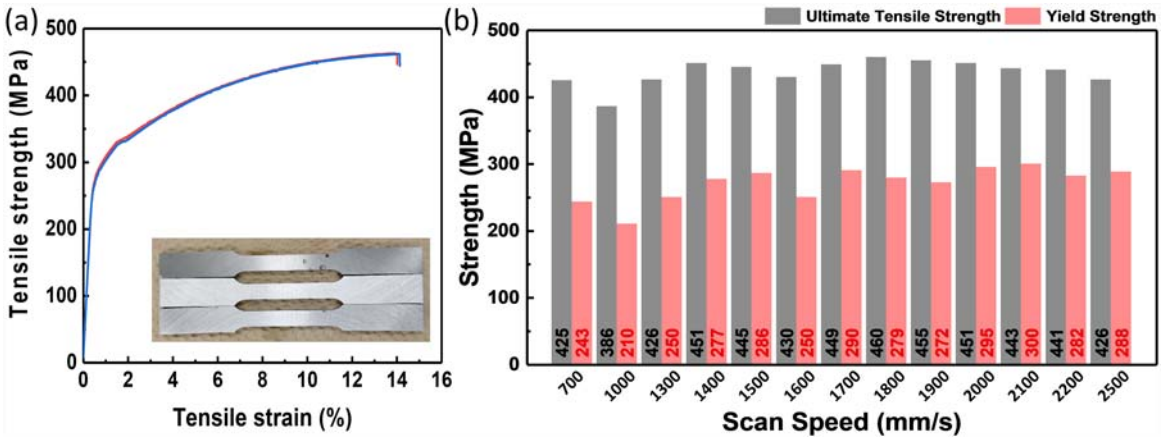

Figure 5. (a) Stress–strain curves of the fabricated sample with laser power of 360 W and scan speed of 1800 mm·s^{-1} (b) variation in tensile strengths of the 3D-printed samples with laser scan speeds.

microstructure, it is not a direct factor that greatly affects tensile strength.

Figure 6(a) shows the results of tensile tests to the sample with the processing condition of 360 W and 1800 mm·s^{-1} after heat treatment at 270, 300, and 330 °C. Tensile strength and yield strength gradually decreased as the heat treatment temperature increased from 270 °C to 330 °C. Figure 6(b) shows the elongation of samples of the laser power of 360 W and the scan speed of 1800, 1900 mm·s^{-1}. As the heat treatment temperature increased, the elongation continued to increase, reaching 15% at 330 °C. Residual stresses caused by rapid melting and solidification reduce the elongation of the AlSi10Mg alloy. As these residual stresses are removed through heat treatment, the elongation seems to increase. Interestingly, it should be noted that the elongation decreased from 9.4% to 5.6% at the sample of 360 W and 1800 mm·s^{-1}. These results indicate that the elongation of 3D-printed samples is affected by the stress-relief heat treatment. This change is planned to be studied later through a more detailed analysis.

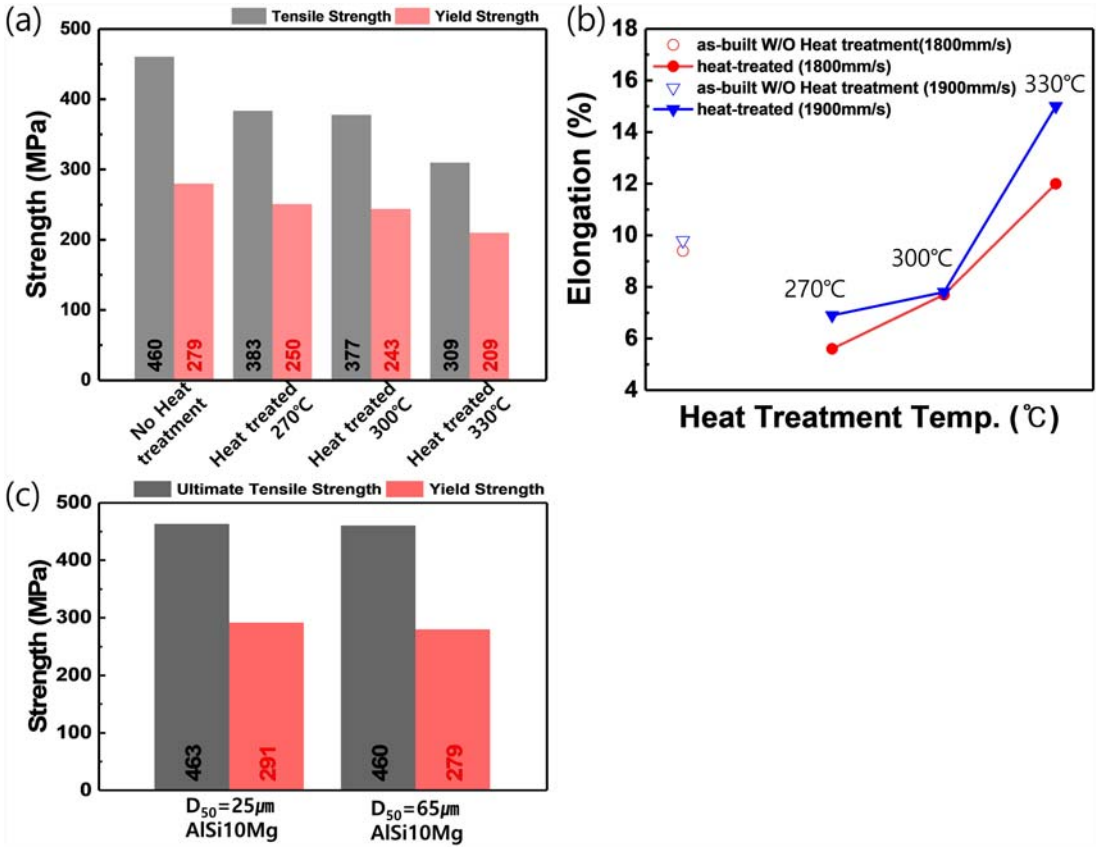

Figure 6. (a) Comparison of strengths with stress-relief heat treatment temperature to as-built specimen made by condition of 360 W and 1800 mm·s^{-1} (b) Variation of elongations of the sample as a function of heat treatment temperatures in both 1800 and 1900 mm·s^{-1} at 360 W, (c) comparison of tensile strengths between two bulk samples using coarse and fine AlSi10Mg powders.

Furthermore, when tensile strengths are compared according to the powder size, the value of the highest mechanical strength is similarly evaluated as shown in Figure 6(c) along with the data from the previous study [18]. The tensile strength of the D_{50} size 25 and 65 μm AlSi10Mg powder is 463 and 460 MPa, respectively, which is not significantly different. In terms of mechanical performance, it was confirmed that there was no significant difference from the previously used powder. Therefore, like scan speed, powder size is related to process optimisation and tensile strength appears to be determined by composition, relative density, microstructure, etc. Nevertheless, since coarse AlSi10Mg powders used in this study provide superior rapid scan speed about 1800 $mm{\cdot}s^{-1}$ compared to that of fine powders, it is expected that the developed powders is profitable in viewpoint of productivity for practical application.

4. Conclusion

Highly flowable AlSi10Mg powders are successfully synthesised by gas atomisation process in this study. The powders are additively manufactured to cube-shaped samples with various processing parameters according to variation of the laser power and scan speed. The optimised SLM processing area for the highly densified AlSi10Mg alloys was achieved and particularly, the developed condition at laser power of 360 W and laser scan speed about 1800 $mm{\cdot}s^{-1}$ provides sound samples. Then, the mechanical properties such as strengths and elongations of the samples are also characterised with the stress-relief heat treatment. When the laser power is 360 W, overall mechanical performance is comparable to that of other studies. Resultantly, although the size of AlSi10Mg powder becomes coarse, it is confirmed that rapid printing is possible compared to printing speed of fine powders due to superior flowability in the bed in SLM process. These results can be utilised as fundamental information for additive manufacturing of coarse Al–Si-based alloy powders.

Acknowledgements

This study was supported by the R&D project entitled 'Development for car body lightweighting and material localisation using 3D Printing technology (Project No: 20004486)' by the Ministry of Trade, Industry and Energy of the Republic of Korea.

Notes on contributors

Yeong Seong Eom is currently working as a Ph.D. student at the Department for 3D Printing Materials, Korea institute of Materials Science, Korea.

Kyung Tae Kim is currently working as a senior researcher at the Department for 3D Printing Materials, Korea institute of Materials Science, Korea. His main research activity is devoted to surface science, powder metallurgy and additive manufacturing.

Dong Won Kim is currently working as a senior researcher at the Department for 3D Printing Materials, Korea institute of Materials Science, Korea. His main research activity is devoted to surface science, powder metallurgy and additive manufacturing.

Soo ho Jung is currently working as a senior researcher at the Department for 3D Printing Materials, Korea institute of Materials Science, Korea. His main research activity is devoted to surface science, powder metallurgy and additive manufacturing.

Jung Woo Nam is currently working as a M.E. student at the Department for 3D Printing Materials, Korea institute of Materials Science, Korea.

Dong Yeol Yang is currently working as a senior researcher at the Department for 3D Printing Materials, Korea institute of Materials Science, Korea. His main research activity is devoted to surface science, powder metallurgy and additive manufacturing.

Jungho Choe is currently working as a researcher at the Department for 3D Printing Materials, Korea institute of Materials Science, Korea. His main research activity is devoted to surface science, powder metallurgy and additive manufacturing.

Ji Hoon Yu is currently working as a senior researcher at the Department for 3D Printing Materials, Korea institute of Materials Science, Korea. His main research activity is devoted to surface science, powder metallurgy and additive manufacturing.

Injoon Son is currently a full professor at the Department of Metallurgical Engineering, Kyungpook National University, Korea.

Disclosure statement

No potential conflict of interest was reported by the author(s).

Funding

This work was supported by Ministry of Trade, Industry and Energy (KR): [Grant Number 20004486].

References

[1] Shin GH, Choi JP, Kim KT, et al. Study on microstructures and hardness of STS316L fabricated by selective laser melting. J Korean Powder Metall Inst. 2017;24:210–215.

[2] Ambrosi A, Pumera M. 3D-printing technologies for electrochemical applications. Chem Soc Rev. 2016;45:2740–2755.

[3] Thijs L, Verhaeghe F, Craeghs T, et al. A study of the microstructural evolution during selective laser melting of Ti–6Al–4 V. Acta Mater. 2010;58:3303–3312.

[4] Attar H, Prashanth KG, Chaubey AK, et al. Comparison of wear properties of commercially pure titanium prepared by selective laser melting and casting processes. Mater Lett. 2015;142:38–41.

[5] Suryawanshi J, Prashanth KG, Scudino S, et al. Simultaneous enhancements of strength and toughness in an Al-12Si alloy synthesized using selective laser melting. Acta Mater. 2016;115:285–294.

[6] Nandwana P, Elliott AM, Siddel D, et al. Powder bed binder jet 3D printing of Inconel 718: densification, microstructural evolution and challenges. Curr Opin Solid State Mater Sci. 2017:21(4):207–218.
[7] Aboulkhair NT, Maskery I, Tuck C, et al. The microstructure and mechanical properties of selectively laser melted AlSi10Mg: The effect of a conventional T6-like heat treatment. Mater Sci Eng A. 2016;667:139–146.
[8] Li XP, Ji G, Chen Z, et al. Selective laser melting of nano-TiB 2 decorated AlSi10Mg alloy with high fracture strength and ductility. Acta Mater. 2017:129:183–193.
[9] Martin JH, Yahata BD, Hundley JM, et al. 3D printing of high-strength aluminium alloys. Nature. 2017;549:365–369.
[10] Kim HT, Kil SC. High efficient Welding technology of the Car bodies. J Welding Joining. 2016;34:62–66.
[11] Read N, Wang W, Essa K, et al. Selective laser melting of AlSi10Mg alloy: process optimisation and mechanical properties development. Mater Des. 2015;65 (1980-2015):417–424.
[12] Louvis E, Fox P, Sutcliffe CJ. Selective laser melting of aluminium components. J Mater Process Technol. 2011:211(2):275–284.
[13] Aboulkhair NT, Everitt NM, Ashcroft I, et al. Reducing porosity in AlSi10Mg parts processed by selective laser melting. Addit Manuf. 2014;1–4:77–86.
[14] Gao C, Liu Z, Xiao Z, et al. Effect of heat treatment on SLM-fabricated TiN/AlSi10Mg composites: Microstructural evolution and mechanical properties. J Alloys Compd. 2021;853:156722–156727.
[15] Liu Y, Wang R, Peng C, et al. Microstructural evolution and mechanical performance of in-situ TiB2/AlSi10Mg composite manufactured by selective laser melting. J Alloys Compd. 2021;853:157287–157297.
[16] Tahiri H, Mohamed SS, Doty HW, et al. Effect of Sr–grain refining–Si interactions on the Microstructural characteristics of Al–Si hypoeutectic alloys. Int J Metalcast. 2017;12(2):343–361.
[17] Fatahalla N, Hafiz M, Abdulkhalek M. Effect of microstructure on the mechanical properties and fracture of commercial hypoeutectic Al-Si alloy modified with Na, Sb and Sr. J Mater Sci. 1999;34:3555–3564.
[18] Lee GS, Eom YS, Kim KT, et al. Microstructures and Characterization of Al-Si-Mg alloy processed by selective laser melting with post-heat-treatment. J Korean Powder Metall Inst. 2019;26:138–145.
[19] Girelli L, Tocci M, Gelfi M, et al. Study of heat treatment parameters for additively manufactured AlSi10Mg in comparison with corresponding cast alloy. Mater Sci Eng A. 2019;739:317–328.